Journal of Histochemistry & Cytochemistry 61(12) 889–900
© The Author(s) 2013
Reprints and permissions:
sagepub.com/journalsPermissions.nav
DOI: 10.1369/0022155413503661
jhc.sagepub.com
SAGE

The *Compact* Mutation of Myostatin Causes a Glycolytic Shift in the Phenotype of Fast Skeletal Muscles

Júlia Aliz Baán, Tamás Kocsis, Anikó Keller-Pintér, Géza Müller, Ernő Zádor, László Dux, and Luca Mendler

Institute of Biochemistry, Faculty of General Medicine, University of Szeged, Dóm tér 9., 6720 Szeged, Hungary (JAB, TK, AKP, EZ, LD, LM); and Egis Pharmaceuticals, H-1475 Budapest, Hungary (GM).

Summary

Myostatin is an important negative regulator of skeletal muscle growth. The hypermuscular *Compact* (*Cmpt*) mice carry a 12-bp natural mutation in the myostatin propeptide, with additional modifier genes being responsible for the phenotype. Muscle cellularity of the fast-type tibialis anterior (TA) and extensor digitorum longus (EDL) as well as the mixed-type soleus (SOL) muscles of *Cmpt* and wild-type mice was examined by immunohistochemical staining of the myosin heavy chain (MHC) proteins. In addition, transcript levels of MHC isoforms were quantified by qPCR. Based on our results, all investigated muscles of *Cmpt* mice were significantly larger compared with that of wild-type mice, as characterized by fiber hyperplasia of different grades. Fiber hypertrophy was not present in TA; however, EDL muscles showed specific IIB fiber hypertrophy while the (I and IIA) fibers of SOL muscles were generally hypertrophied. Both the fast TA and EDL muscles of *Cmpt* mice contained significantly more glycolytic IIB fibers accompanied by a decreased number of IIX and IIA fibers; however, this was not the case for SOL muscles. In summary, despite the variances found in muscle cellularity between the different myostatin mutant mice, similar glycolytic shifts were observed in *Cmpt* fast muscles as in muscles from myostatin knockout mice. (J Histochem Cytochem 61:889–900, 2013)

Keywords

myostatin, *Compact* mice, muscle, tibialis anterior, extensor digitorum longus, soleus, hyperplasia, hypertrophy, myosin heavy chain, fiber type transition

1. Introduction

Myostatin, also known as growth/differentiation factor 8 (GDF-8) is a member of the transforming growth factor (TGF)-β superfamily and has been shown to be a negative regulator of skeletal muscle growth. The myostatin knockout (KO) mouse (McPherron et al. 1997) shows a hypermuscular phenotype similar to that of several different organisms (cattle, dog, pig, sheep, human) carrying naturally occurring mutations of myostatin (McPherron and Lee, 1997; Schuelke et al. 2004; Clop et al. 2006; Mosher et al. 2007; Stinckens et al. 2008). Most of the natural mutations result in an inactive protein caused by either an early STOP codon or a frameshift mutation in the bioactive domain of myostatin (McPherron and Lee, 1997; Mosher et al. 2007, Boman et al. 2009). One report details that missplicing of the myostatin pre-mRNA was responsible for hypermuscularity observed in a human infant (Schuelke et al. 2004). In contrast, another mechanism of myostatin inactivation induces the hypermuscular phenotype of the *Compact (Cmpt)* mice, which was originally selected for high protein content and body weight in the Technical

Received for publication March 22, 2013; accepted August 1, 2013.

Supplementary material for this article is available on the *Journal of Histochemistry & Cytochemistry* Web site at http://jhc.sagepub.com/supplemental.

Corresponding Author:
Luca Mendler MD PhD, Institute of Biochemistry, Faculty of General Medicine, University of Szeged, Dóm tér 9., 6720 Szeged, Hungary.
E-mail: mendler.luca@med.u-szeged.hu

University of Berlin (Bünger et al. 2001). Analysis of the Hungarian inbred subpopulation of the *Cmpt* line identified myostatin as the major gene containing a 12-bp non-frameshift deletion in the propeptide region, although the biologically active part of the molecule was unaffected (Varga et al. 1997). Additional modifiers seem to be essentially involved in determining the full expressivity of the *Cmpt* phenotype; however these genes have not been identified yet (Szabó et al. 1998; Varga et al. 2003, 2005). To date, few studies describe the phenotypical or molecular analysis of the *Cmpt* mice (Bünger et al. 2004; Rehfeldt et al. 2005; Amthor et al. 2007, 2009), even though this line represents, in contrast to myostatin KO, a complex and mainly unknown mechanism of myostatin-dependent hypermuscularity.

Various contradictory results exist in the literature regarding muscle cellularity in myostatin-deficient mice. Thus, in the present study, we aimed to describe the muscle phenotype of young male *Cmpt* mice using morphological assessments. By analyzing the fast-type tibialis anterior (TA) and extensor digitorum longus (EDL) as well as the mixed-type soleus (SOL) muscles, we show here that hypermuscularity is characterized by either muscle fiber hyperplasia or combined hyperplasia and hypertrophy of different grades depending on muscle type, and that a significant glycolytic shift occurs in the fiber type composition of the fast-type muscles of *Cmpt* mice.

2. Materials and Methods

2.1 Animals

The genetic background of BEHi (Berlin High inbred) line is not well defined because it was derived from an out-bred line founded from mice bought from pet shops more than 40 years ago (Bünger et al. 2001). It was initially selected on protein mass (Weniger et al. 1974), then on high body weight/low fat content (Valle Zarate et al. 1994) and finally on body weight (Bünger et al. 2004). The '*Compact'* line in Berlin was derived from the first mice seen in early generations of the BEH line showing this phenotype, and were separated to form a new line that was selected on a muscularity score by visual inspection (Szabó et al. 1998; Varga et al. 2003, 2005). Animals of the Berlin *Cmpt* line were used as the founders for the Hungarian *Cmpt* line, and there was no further exchange of genetic material between the laboratories in Berlin and Hungary. The Hungarian subpopulation of the *Cmpt* mice was inbred and kept by Géza Müller until 2010 in the Institute for Animal Biology, Agricultural Animal Center, H-2101 Gödöllő, Hungary, and in EGIS Pharmaceuticals, Budapest, Hungary. Since 2010, these mice have been kept in the Institute of Biochemistry, Faculty of General Medicine, University of Szeged, Hungary.

BALB/c mice, serving as wild-type control for the experiments, were purchased from Biological Research Centre of Szeged, Hungary.

2.2. Experimental Design

Male, 2.5-month (10–12-week)-old *Cmpt* (44-50.7 g) and BALB/c (24-28g) wild-type mice were used for the experiments (n=5–10). Typical hindlimb muscles (quadriceps (Quadr), tibialis anterior (TA), extensor digitorum longus (EDL), soleus (SOL) and gastrocnemius (Gastro)) of both strains were removed under intraperitoneal anesthesia (3% chloral hydrate, 0.15 ml/10 g body weight). Older male *Cmpt* mice (4-, 7-, 12-, 18-, and 23-month-old) were also used for comparison of body and muscle weight, as well as for some fiber analyses of TA muscles. All muscles were weighed and frozen in isopenthane/liquid nitrogen and kept at -80C until further use. TA, EDL and SOL muscles from the right leg were used for morphological and immunohistochemical analysis while RNA isolation and quantitative RT-PCR was carried out on the contralateral TA counterparts. Animal experiments were approved by the Institutional Animal Care and Use Committee at the University of Szeged in accordance with the U.S. National Institutes of Health guidelines for animal care.

2.3. Morphological Analysis

For morphological analysis, 10-μm serial cryostat sections were taken from the mid-belly region of different muscles of both *Cmpt* and BALB/c mice followed by standard hematoxylin-eosin (HE) staining. Using images from all microscopic fields, we reconstructed the whole cross-sectional area (CSA) of each muscle using the Cell B program (Olympus DP Soft software, Version 3.2., Soft Imaging System GmbH; Münster, Germany) and fiber number was determined by counting all fibers in TA, EDL and SOL muscles using Digimizer software (MedCalc Software, Mariakerke, Belgium).

2.4. Myosin Heavy Chain (MHC) Immunohistochemistry

Fiber type analysis was carried out on 10-μm thick serial cryosections of TA, EDL and SOL muscles from both *Cmpt* and BALB/c wild-type male mice. Sections were first blocked in 5% non-fat milk powder in PBS, then incubated with mouse monoclonal primary antibodies BA-D5 (1:25), sc-71 (1:25) and BF-F3 (1:5), which are specific for myosin heavy chain (MHC) I (slow oxidative) MHCIIA (fast oxidative) and MHCIIB (fast glycolytic), respectively (Deutsche Sammlung von Mikroorganismen und Zellkulturen [DSMZ], Braunschweig, Germany). After incubation with the peroxidase-conjugated secondary antibody (rabbit anti-mouse; Dako, Denmark) immunocomplexes were visualized by diaminobenzidine (DAB) staining with or without nickel enhancement. IIX fibers were considered as those not stained by any of the above antibodies. The size and distribution of muscle fibers in SOL were determined by analyzing all

Table 1. Primer sequences of different MHC isoforms and Hprt used in qRT-PCR.

Target	Accession number	Forward primer	Reverse primer	Product size (bp)
MHCIIB	NM_010855.2	GTGATTTCTCCTGTCACCTCTC	GGAGGACCGCAAGAACGTGCTGA	280
MHCIIX	NM_030679.1	ACGGTCGAAGTTGCATCCC	CAGTAGTTCCGCCTTCGGTC	272
MHCIIA	NM_001039545.2	TGCACCTTCTCGTTTGCCAG	GGCCATGTCCTCGATCTTGT	320
MHCI	NM_003689292.1	CTACAGGCCTGGGCTTACCT	TCTCCTTCTCAGACTTCCGC	126
Hprt	NM_013556.2	TCAGTCAACGGGGGACATAAA	GGGGCTGTACTGCTTAACCAG	142

bp: base pair; MHC: myosin heavy chain; Hprt: Hypoxanthine guanine phosphorybosyltransferase.

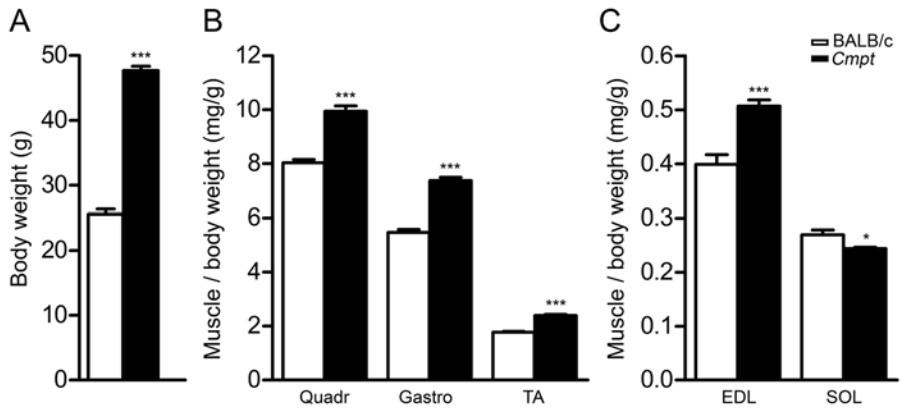

Figure 1. Body weight (A) and normalized muscle mass (B, C) of BALB/c and *Cmpt* male mice. B-C show normalized muscle masses of quadriceps (Quadr), gastrocnemius (Gastro), tibialis anterior (TA), extensor digitorum longus (EDL) and soleus (SOL) muscles. Bars represent mean ± SEM; asterisks show significant differences between BALB/c and *Cmpt* mice (n=5-10, *p<0.05, ***p<0.001).

(700-800) fibers in each muscle using Cell B and Digimizer software; in EDL muscles, about 50% of the fibers (600 to 1100 fibers in BALB/c and *Cmpt* mice, respectively) were measured. In TA muscles, an analysis of fiber size as well as fiber type distribution was done by examining 2-3 representative microscopic fields (with 10x objective) of both superficial and deep portions of TA muscles. Regional results were then summarized for the whole cross-sectional area of each TA muscle (500 to 1000 fibers/muscle in 4-7 microscopic fields in BALB/c and *Cmpt* mice, respectively).

2.5. Quantitative RT-PCR Analysis

Total RNA was isolated from TA muscles of *Cmpt* and BALB/c male mice (n=5) with TRI reagent according to the manufacturer's instructions (Molecular Research Center, Inc. Cincinnati, OH), followed by reverse transcription (MMLV-Moloney Murine Leukemia Virus Reverse Transcriptase, 28025-013, Sigma-Aldrich, St. Louis, MO). For the detection of transcript levels of MHCI, MHCIIA, MHCIIX and MHCIIB, quantitative PCR was carried out with SYBR GREEN master mix (Fermentas, Thermo Fischer Scientific, Pittsburgh, PA) on a Light Cycler 1.5 (Roche Applied Science, Indianapolis, IN). As an internal control, *Hprt* (hypoxanthine guanine phosphorybosyltransferase) was amplified using the same TA muscle probes. Cycle conditions were set as an initial denaturation step for 10 min at 95C, followed by 45 cycles of 10 sec at 95C for template denaturation, 10 sec at 58C for annealing phase and 10 sec at 72C for extension. Specificity of the PCR products was confirmed by melting curve analysis followed by verification of the amplicon length on 1.5% agarose gels stained with ethidium bromide. Primer pairs for *Hprt*, MHCI, MHCIIA, MHCIIX and MHCIIB were designed against sequences of intron-spanning exons by Primer 3 Input software (version 0.4.0; http://frodo.wi.mit.edu/primer3/input.htm) and tested to avoid primer dimers, non-specific amplification and self-priming (Table 1).

2.6. Statistical Analysis

Statistical analysis was performed by unpaired t test using Prism software (GraphPad Software, Inc.; San Diego, CA). Age-dependent body and muscle weights of *Cmpt* mice (Fig. S1) were tested using a one-way ANOVA and Newman-Keuls multiple comparison tests. All data are expressed as the mean ± SEM. The level of p<0.05 was considered significant. The individual p-values are indicated in the legends to each figure.

3. Results

3.1. Body and Muscle Weight of Cmpt *Mice*

We phenotypically compared 2.5-month-old myostatin mutant *Cmpt* mice (Varga et al. 1997) with wild-type BALB/c mouse using scores of body and muscle weight. *Cmpt* male mice were significantly larger than BALB/c mice in terms of body weight (Fig. 1A). Absolute weights

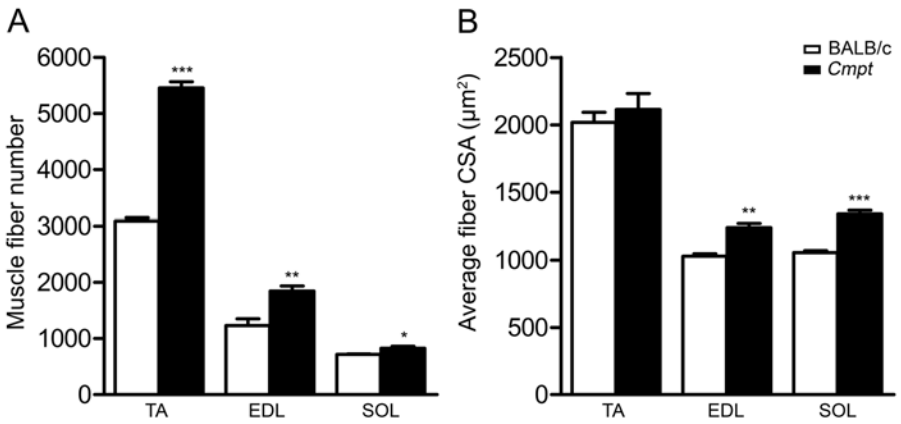

Figure 2. Total muscle fiber number (A) and average fiber cross-sectional area (CSA) (B) of tibialis anterior (TA), extensor digitorum longus (EDL) and soleus (SOL) muscles in BALB/c and *Cmpt* male mice. Bars represent the mean ± SEM; asterisks show significant differences between BALB/c and *Cmpt* mice (n=3-5, *p<0.05, **p<0.01, ***p<0.001).

of the different hindlimb muscles, such as Quadr, Gastro, TA, EDL and SOL muscles, were significantly larger in *Cmpt* mice (data not shown). Similarly, muscle weights, normalized to body weights, were significantly larger in *Cmpt* animals, with the exception of the oxidative SOL muscle. These results indicated a disproportionate increase in mass for most muscles of *Cmpt* mice (Fig. 1B-C). To assure that the 2.5-month-old *Cmpt* mice had already finished the intense growing phase, we compared body and muscle (TA, EDL and SOL) weights in mice of different ages (Fig. S1). Body weight was similar in young (2.5-month-old) and adult (4- and 7-month-old) animals, while 12–23-month-old mice had slightly higher weight measurements. However, no significant difference was found in muscle weights amongst any of the age groups, indicating that the 2.5-month-old animals we used for the experiments have already reached muscle sizes typical of adult mice.

3.2. Muscle Fiber Number and Fiber Cross-sectional Area

To define whether the hypermuscularity of *Cmpt* mice is caused by hyperplasia or hypertrophy within the muscle, we analyzed muscle fibers on HE- or MHC-immunostained serial cross-sections of different muscle types—glycolytic TA and EDL muscles and oxidative SOL muscles—in both mutant and wild-type groups (Fig. 2). Fiber number in all examined muscles of the 2.5-month-old *Cmpt* mice was significantly higher than that observed in wild-type mice. The TA muscle demonstrated the most significant hyperplasia as compared with the EDL and SOL muscles (Fig. 2A). However, fiber size did not differ in TA muscles between *Cmpt* and BALB/c mice. EDL and SOL muscles of *Cmpt* mice, on the other hand, showed evidence of hypertrophy (Fig. 2B). To check whether older *Cmpt* mice also show changes in fiber parameters, we analyzed TA muscles of 7-month-old *Cmpt* mice and found no differences in mean fiber number or size compared with the 2.5-month-old *Cmpt* mice (fiber number: 5450 ± 135 vs. 5455 ± 114; fiber size: 2193 ± 95 vs. 2114 ± 118, respectively) (Table S1). In summary, based on our results, hypermuscularity of *Cmpt* mice is characterized by fiber hyperplasia in TA muscles and by a combination of hyperplasia and different grades of hypertrophy in EDL and SOL muscles.

3.3. MHC Composition and Fiber Size Distribution

To analyze the possible effects of the *Cmpt* mutation on MHC composition, serial cryosections of TA, EDL and SOL muscles were immunostained using sets of monoclonal antibodies in order to differentiate type I, IIA, IIX and IIB fibers (Figs. 3-6). In line with the literature (Bloemberg et al. 2012), only MHCII isoforms were detected in TA and EDL muscles of both mouse lines (Figs. 3-6). Whereas, no MHCIIB fibers were found in SOL muscles. Therefore, we next analyzed the parameters of the slow-type I and the fast-type IIA and IIX fibers in SOL muscles (Figs. 3-6).

By counting different fiber types on whole cross-sectional images, we noted that the fast-type TA muscles of *Cmpt* mice contained significantly more glycolytic IIB fibers and a decreased number of IIX and IIA fibers as compared with that in wild-type mice (Fig. 3, 4, 5A). Fiber composition has been shown to be different in superficial and deep portions of TA muscles in wild-type mice, with more glycolytic IIB fibers at the periphery (Bloemberg et al. 2012). Therefore, we also compared the regional fiber type composition in both mouse lines (Fig. 4, 5B). The number of IIB fibers was significantly higher in both superficial and deep regions of *Cmpt* mice compared with that in wild-type animals (Fig. 4, 5B). Moreover, in *Cmpt* mice, both muscle regions contained a similar number of IIB fibers, whereas, in wild-type BALB/c mice, the IIB fibers were abundant only in the superficial region, as expected (Fig. 4, 5B). In contrast, the proportion of the glycolytic-oxidative IIX fibers significantly decreased in both TA regions of *Cmpt* mice, without any regional difference in fiber number

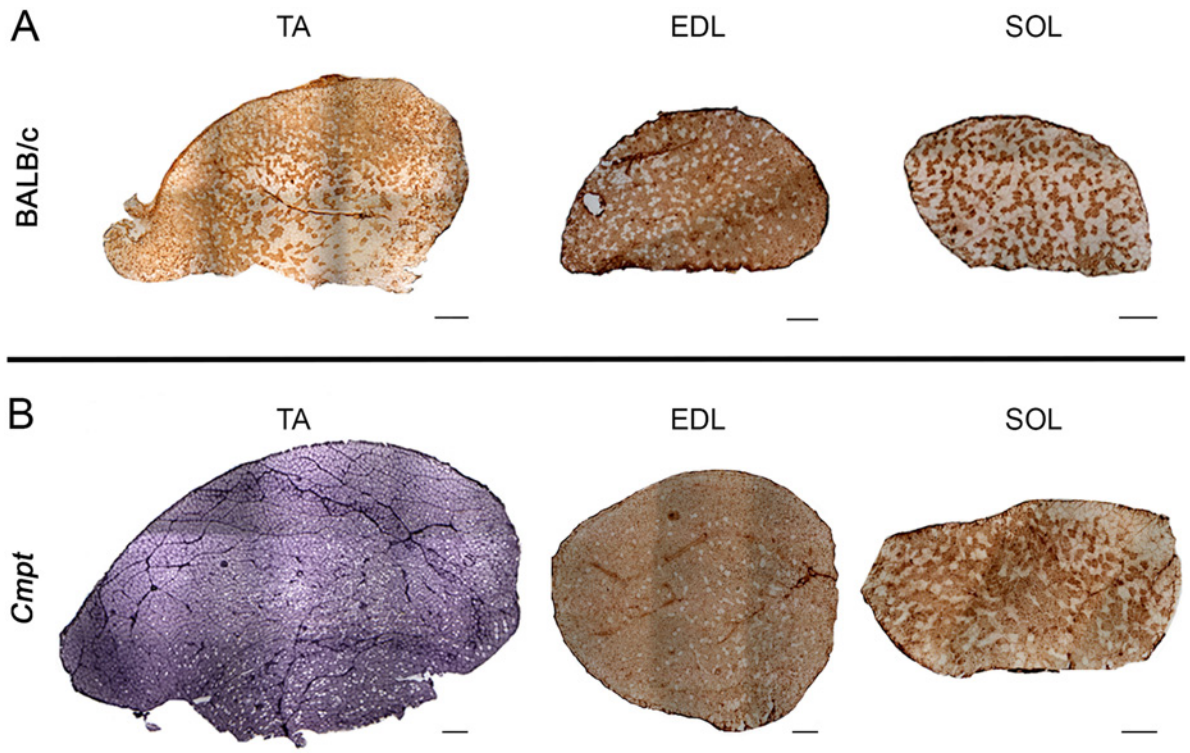

Figure 3. Representative immunohistochemical stainings of tibialis anterior (TA), extensor digitorum longus (EDL) and soleus (SOL) muscles of BALB/c (A) and *Cmpt* (B) male mice. Panel A represents whole cross-sectional areas of TA, EDL and SOL muscles stained either by MHCIIB antibody (in TA and EDL muscles) or by MHCI antibody (in SOL muscle) in BALB/c mice, and panel B shows the same tissue staining for sections from *Cmpt* male mice. All muscles were stained by diaminobenzidine but *Cmpt* TA muscle was additionally nickel enhanced. Scale bars represent 400 µm for TA, 200 µm for EDL and 200 µm for SOL muscles.

(Fig. 4, 5B). In wild-type mice, however, we found a significantly higher proportion of IIX fibers in the deep region (Fig. 4, 5B). Finally, the number of the oxidative IIA fibers was very low, and these were almost exclusively confined to the deep region of TA muscles in both mouse strains; however, the number of IIA fibers was even reduced in *Cmpt* mutant mice compared with wild-type animals (Fig. 4, 5B).

Similar to TA muscles, the number of glycolytic IIB fibers was higher in the fast-type EDL muscles of *Cmpt* mice, while the number of IIX and IIA fibers was significantly lower as compared with that of wild-type mice (Fig. 3, 5A). In contrast, the oxidative SOL muscles in *Cmpt* mice contained more slow-type I fibers and less fast-type IIA fibers than those in wild-type mice, while the number of IIX fibers was very low and not different in the two mouse lines (Fig. 3, 5A).

Together, our findings clearly demonstrate a substantial shift toward a more glycolytic phenotype in the fast-type TA and EDL muscles but not in the mixed-type oxidative SOL muscles of *Cmpt* mice.

In line with our results regarding average fiber size (Fig. 2B), we could not detect any specific hypertrophy for any of the IIB, IIX or IIA fiber types in TA muscles (Fig. 5C). Indeed, the size distribution of the IIB, IIX and IIA fibers in TA muscles revealed only minimal changes in terms of peak position or shape of the histograms in *Cmpt* mice when compared with the results seen for wild-type mice (Fig. 6A). In EDL muscles, however, fiber hypertrophy (Fig. 2B) was exclusively caused by the increased size of IIB fibers, while the sizes of IIX and IIA fibers were unchanged (Fig. 5C). In line with these findings, IIB fiber distribution in EDL muscles was shifted toward larger fiber size in *Cmpt* mice, while IIX and IIA histograms were not different between the *Cmpt* and BALB/c lines (Fig. 6B). In contrast to fast muscles, both I and IIA fibers showed evidence of hypertrophy for *Cmpt* mice (Fig. 5C), such that both fiber frequencies shifted toward an increase in size in *Cmpt* SOL muscles as compared with BALB/c SOL muscles (Fig. 6C). Because of their low number, IIX fiber size was not analyzed in SOL muscles.

3.4. mRNA Levels of MHC Isoforms Detected by Quantitative RT-PCR

In order to determine the transcript levels of MHC isoforms (MHCI, IIA, IIB, IIX), we performed qRT-PCR analysis in TA muscles of both *Cmpt* and BALB/c male mice (Fig. 7).

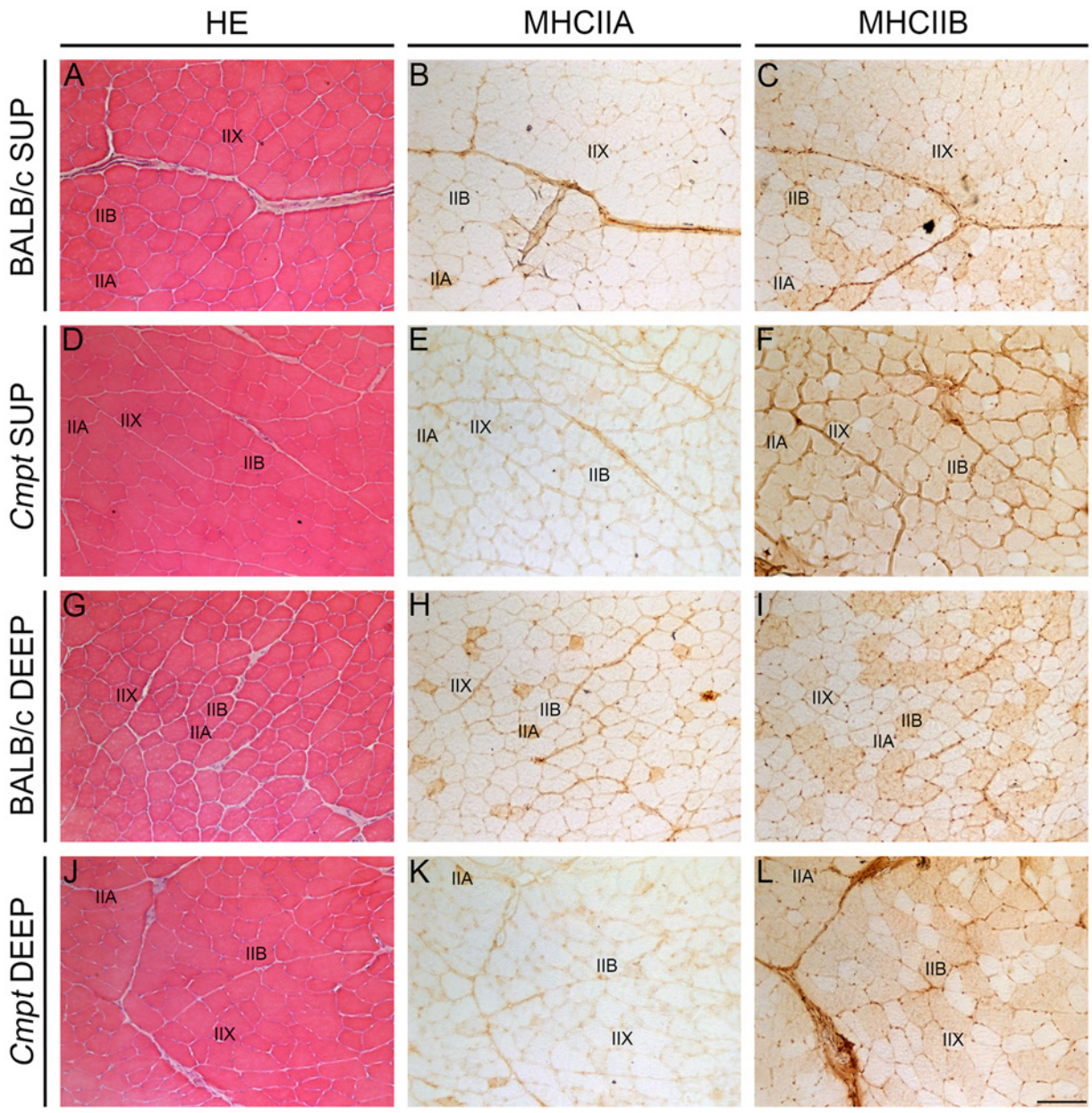

Figure 4. Immunohistochemical analysis of myosin heavy chain (MHC) isoforms in different regions of tibialis anterior (TA) muscles of BALB/c and *Cmpt* male mice. A-C represent the superficial region of BALB/c mice and D-F depict that of *Cmpt* mice; G-I and J-L show BALB/c and *Cmpt* deep regions, respectively. HE staining (A, D, G, J) and antibodies against MHCIIA (B, E, H, K) and MHCIIB (C, F, I, L) were used. Representative fibers are marked as IIA, IIB and IIX fibers. Scale bars represent 100 μm.

Hprt was used as an internal control because *Hprt* levels were similar in *Cmpt* vs. wild-type TA muscles (Fig. 7A). We found that MHCIIB mRNA levels were significantly increased (Fig. 7B), while MHCIIX (Fig. 7C) and MHCIIA transcript levels (Fig. 7D) decreased in *Cmpt* mice compared with those values in wild-type mice. The slow MHCI isoform was almost undetectable (data not shown). These results are in line with those obtained from the immunohistochemical analysis, suggesting that the fiber-type shift in the TA muscle is regulated at the level of MHC transcription.

4. Discussion

The *Cmpt* mouse line takes a special place in the group of hypermuscular animals carrying naturally occurring myostatin mutations, as the propeptide region, not the biologically active domain, of myostatin is affected. Abnormal propeptide structure might play an important role in misfolding, inefficient secretion, and/or abnormal processing of myostatin in *Cmpt* mice (Szabó et al. 1998). It has also been shown that the *Cmpt* mutation of myostatin is an

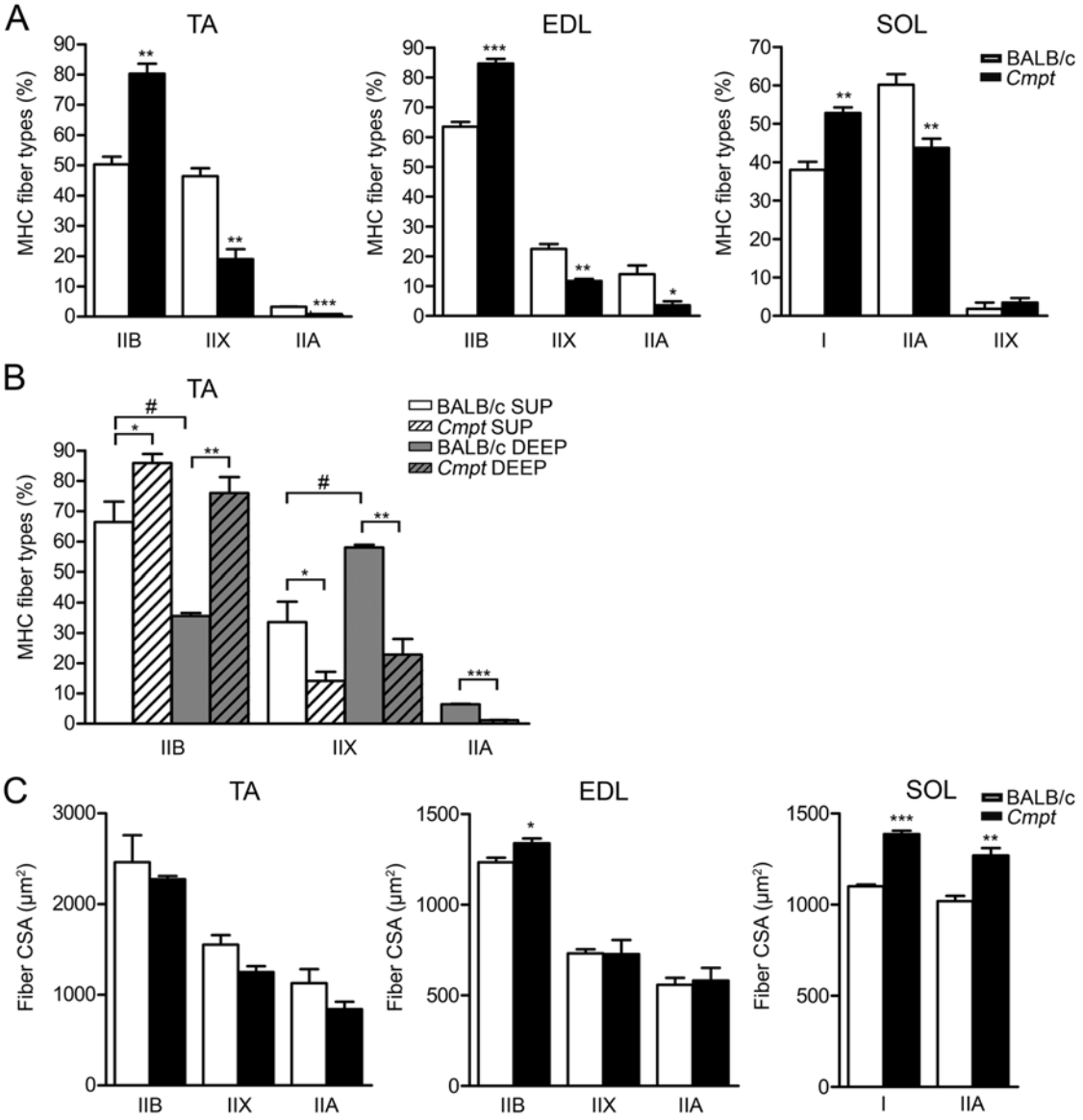

Figure 5. Fiber type composition (A-B) and mean fiber cross-sectional area (C) in tibialis anterior (TA), extensor digitorum longus (EDL) and soleus (SOL) muscles of BALB/c and *Cmpt* male mice. Panel A represents fiber type composition of all fibers in TA, EDL and SOL muscles, while panel B shows regional fiber type distribution of TA muscles subdivided into superficial and deep regions. Panel C represents mean fiber cross sectional area (CSA) of the different (I, IIA, IIX and IIB) fibers in TA, EDL and SOL muscles. Data are presented as the mean ± SEM. Asterisks show significant differences between BALB/c and *Cmpt* mice (n=3–4, *p<0.05, **p<0.01, ***p<0.001) while a crosshatch indicates significant changes between superficial and deep portions of the same TA muscle within a specific mouse line (n=3, $^{\#}p$<0.05).

indispensable yet not satisfactory requirement for the full expression of the hypermuscular phenotype, pinpointing the significance of additional modifier gene or genes (Varga et al. 1997, 2003, 2005).

Since the genetic background of the *Cmpt* mice is very complex and no appropriate genetic control line has been available so far, we decided to use BALB/c mice as a control for the following reasons: 1) This inbred line was used for mapping the myostatin mutation and the modifier genes in *Cmpt* mice (Szabó et al. 1998); 2) These mice are generally used as wild-type controls and their muscle parameters as well as fiber composition have already been reported (Freitas et al. 2002; Luedecke et al. 2004); and 3) Muscle characteristics of BALB/c mice are similar to those of C57BL/6, another wild-type mice used as a genetic background of myostatin KO mice (McPherron et al. 1997), suggesting that these lines are comparable to some extent (Luedecke et al. 2004; Pellegrino et al. 2005; Bloemberg et al. 2012; McKeehen et al. 2013).

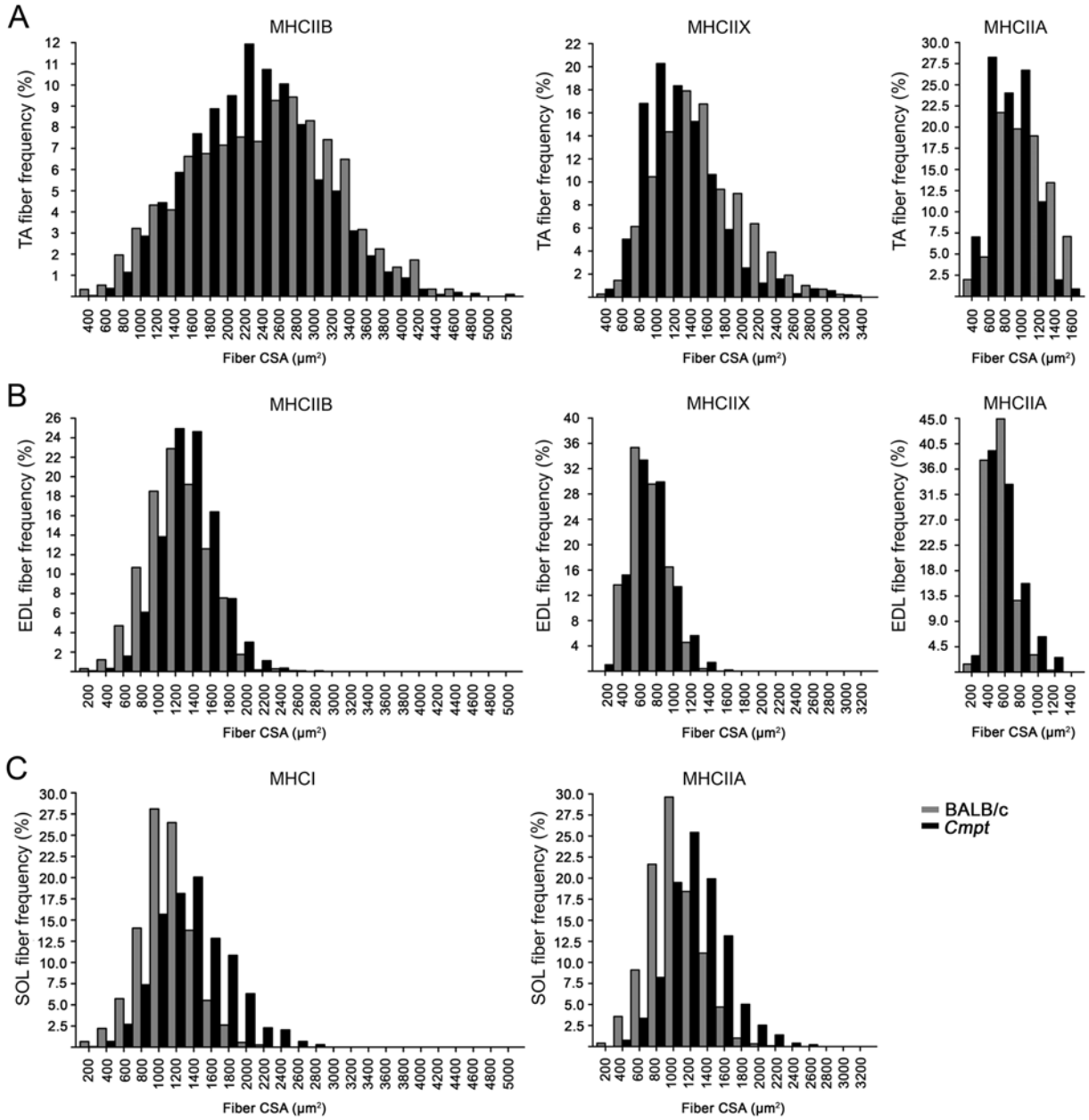

Figure 6. Frequency distribution of fiber size in tibialis anterior (TA) (A), extensor digitorum longus (EDL) (B) and soleus (SOL) (C) muscles of BALB/c and *Cmpt* male mice specific to each myosin heavy chain (MHC) isoform: MHCIIB, MHCIIX, MHCIIA and MHCI. CSA, fiber cross-sectional area.

In the present study we show, in accordance with others (Bünger et al. 2004; Rehfeldt et al. 2005; Amthor et al. 2007, 2009), that body and muscle weights of male *Cmpt* mice are higher than those of wild-type BALB/c mice. Body mass is even higher in *Cmpt* mice (47.7g) than it is described for male myostatin KO of the same age (38–41g) (McPherron et al. 1997). However, muscle weights normalized to body weight are comparable in both myostatin mutant lines, suggesting that *Cmpt* and myostatin KO mice represent a similar grade of muscularity. One exception was the SOL muscle, which seemed to be different in this regard, as its relative muscle-to-body weight did not increase in *Cmpt* compared with the wild-type mice. Indeed, it has been reported earlier that the oxidative SOL muscle contained less myostatin transcripts than the glycolytic EDL muscle (Mendler et al. 2000; Wang et al. 2012) and that the lack of myostatin had a stronger effect on glycolytic muscles than on oxidative ones (McPherron et al. 1997; Carlson et al. 1999; Hennebry et al. 2009; Wang et al. 2012). Therefore, we analyzed three different hindlimb

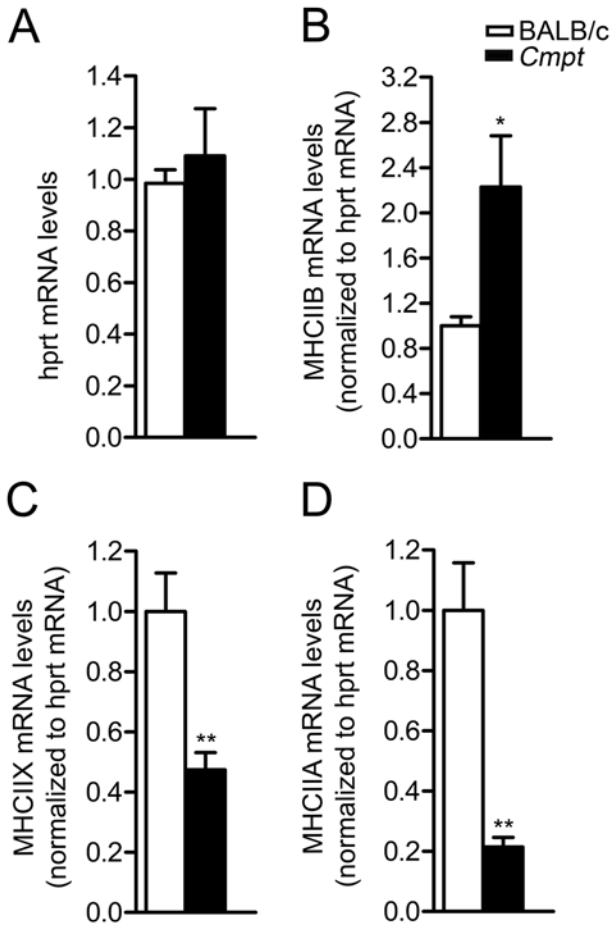

Figure 7. mRNA levels of myosin heavy chain (MHC) isoforms and *Hprt* in TA muscles of BALB/c and *Cmpt* male mice. Bars in B-D represent mRNA levels of MHCII isoforms normalized to *Hprt* transcripts (A). Data are expressed as the mean ± SEM. (n=5, *p<0.05, **p<0.01,).

muscles: the fast-glycolytic TA and EDL as well as the oxidative SOL muscles in *Cmpt* mice.

Based on extensive morphological analyses, measuring and counting all fibers on HE-stained cross sections and 500–1000 fibers on MHCIIB-stained sections, the TA muscles were exclusively characterized by muscle fiber hyperplasia, with an absence of hypertrophy. This observation may be somewhat surprising, as earlier reports described both hyperplasia and hypertrophy in different myostatin KO animals (McPherron and Lee, 1997; Amthor et al. 2009). However, even in the original myostatin KO mouse report (McPherron et al. 1997), the ratio of hyperplasia to hypertrophy varied in the different muscles; *e.g.*, the TA muscles of myostatin KO mice were dominated by hyperplasia, while only 14% fiber hypertrophy was documented. It is worth mentioning that the myostatin KO vs. myostatin$^{+/+}$ control mice (McPherron et al. 1997) contained similar fiber number in TA muscles (5470 vs. 2936) as observed with the *Cmpt* vs. BALB/c mice in our study (5455 vs. 3093), which makes the KO and *Cmpt* experiments somewhat comparable. In contrast to TA, the EDL muscles of *Cmpt* mice were characterized by a combination of hyperplasia (50%) and hypertrophy (20%), whereas, in the myostatin KO, the same type of muscles showed only a moderate hyperplasia and a stronger hypertrophy (Amthor et al. 2009). Amthor and colleagues (2009) compared EDL muscles of KO mice with that of the female 'Berlin' *Cmpt* mice (BEH$^{c/c}$). In line with our findings, they also detected stronger hyperplasia in female BEH$^{c/c}$ EDL muscles (1589) than in the KO (1200). Interestingly, the fiber number of both BEH$^{+/+}$ and myostatin$^{+/+}$ controls were also comparable with ours (1083 and 1160 vs. 1232, respectively). However, our results are somewhat different from those described for the BEH$^{c/c}$ females, for which fiber hypertrophy was very pronounced and still dominated over hyperplasia (Amthor et al. 2009). We found that the moderate fiber hypertrophy in *Cmpt* EDL was confined to the most glycolytic IIB fibers and not to the IIX or IIA fibers. This is again in accordance with the earlier reports that showed a stronger effect of myostatin on glycolytic muscles (McPherron et al. 1997; Carlson et al. 1999; Hennebry et al. 2009; Wang et al. 2012). We believe that the long separation of the 'Berlin' and Hungarian *Cmpt* lines, gender differences, the use of different controls as well as the higher number of fibers analyzed in our experiments (3000/1800 fibers in *Cmpt*/BALB/c vs. 150/180 fibers in BEH$^{c/c}$ /BEH$^{+/+}$ (Amthor et al. 2009) may account for these differences.

In the oxidative SOL muscle of *Cmpt* mice, low-grade hyperplasia (15%) and mainly hypertrophy (27%) accounted for the moderately higher mass of the mice as compared with wild-type mice. Moreover, both the oxidative I and IIA fibers showed evidence of hypertrophy compared with the wild-type mice. The changes in SOL are quite different from those of fast TA and EDL muscles in the *Cmpt* line and it is also difficult to compare them to myostatin KO mice where either 32% hyperplasia (Girgenrath et al. 2005) or 20% fiber hypertrophy has previously been described (Gentry et al. 2011).

It is not known so far, how cellularity in different muscle types is regulated upon myostatin defect. However, prenatal hyperplasia seems to be the major effect of developmental myostatin deficiency in most muscles of mice and cattle (McPherron et al. 1997; Grobet et al. 1997; Lee and McPherron 1997). Based on the different ratio of hyperplasia to hypertrophy in various myostatin-deficient muscles, myostatin might have a strong, but muscle type-dependent, effect on the proliferation of muscle precursor cells. Consequently, postnatal fiber hypertrophy might be restricted to different grades. Rehfeldt and co-workers (2005) introgressed the myostatin mutant *Cmpt* allele into a special high-growth mouse line (DUHi) and detected,

similar to our results, muscle hyperplasia in the predominantly fast rectus femoris and longissimus dorsi muscles, without any muscle hypertrophy. These data suggest that, at least in fast muscles, hyperplasia is even more pronounced in *Cmpt* mice than in myostatin KO mice. The difference might reside in the allelic variation of the myostatin defect and/or in modifier genes influencing *Cmpt* phenotype. To show that the dominance of hyperplasia (over hypertrophy) found in 2.5-month-old *Cmpt* muscles is not the result of delay in postnatal fiber growth, we analyzed TA muscles of 7-month-old *Cmpt* male mice. We found a similar hyperplasia without any substantial fiber hypertrophy in these older animals, which refutes that the increase of fiber size might reach its peak later in adulthood in *Cmpt* mice.

Although TA and EDL muscles contain predominantly type II glycolytic fibers (Bloemberg et al. 2012), we observed a significant glycolytic shift within type II fibers in *Cmpt* compared with wild-type mice. This result again is consistent with that of Rehfeldt et al. (2005) who found more glycolytic fibers in the rectus femoris muscle of the special *Cmpt*-DUHi line by NADH-tetrazolium reductase staining. A substantial glycolytic shift was also described in EDL muscles of myostatin KO mice as well as in double-muscled cattle using different methods (ATPase and SDH staining vs. immunohistochemical analysis), showing that both metabolic and structural protein changes occur with a myostatin deficiency (Wegner et al. 2000; Girgenrath et al. 2005; Amthor et al. 2007). However, immunohistochemical staining of MHC isoforms used in our study is more appropriate to distinguish between fiber types. By this method, significantly more IIB fibers and less IIX or IIA fibers were detected in TA muscles of *Cmpt* mice than in wild-type mice. Moreover, we analyzed fiber type distribution in superficial and deep portions of TA, as there are regional differences in glycolytic fibers distribution in wild-type mice (Bloemberg et al. 2012). Interestingly, the regional difference disappeared in *Cmpt* mice in contrast to wild-type, so that both superficial and deep regions of TA muscles were dominated by the glycolytic IIB fibers of a quite uniform fiber size. Transcript levels were in agreement with our immunohistochemical results: MHCIIB mRNA levels were significantly higher, while those of MHCIIX and IIA significantly lower in *Cmpt* TA muscles compared with those genes in wild-type muscles. These findings suggest that the fiber–type shift in fast muscles detected in our study is supported at the level of both MHC transcripts and proteins.

Likewise, we measured the same ratio of IIB/IIX/IIA fibers in EDL muscles of *Cmpt* mice using immunohistochemical methods, as performed by Amthor and colleagues (2007) for myostatin KO mice. The results shows that, in fast skeletal muscles, the *Cmpt* mutation results in similar glycolytic changes as the complete lack of myostatin protein in the KO mice. The glycolytic shift was consistent with the decrease in mitochondrial content, a reduced expression of cytochrome c oxidase, a lower citrate synthase activity and a shortening of contraction as well as relaxation time in myostatin KO mice (Amthor et al. 2007; Savage and McPherron 2010). Moreover, KOs showed impaired tolerance to chronic repetitive contractions (Ploquin et al. 2012) and a decrease in specific force generation, similar to that which was measured in $BEH^{c/c}$ female EDL muscles (Amthor et al. 2007). These data suggest that the function of the bigger and more glycolytic muscles is impaired upon myostatin defect.

However, the oxidative SOL muscles did not show any glycolytic shift in *Cmpt* mice in our experiments (53% slow-oxidative type I fibers, 44% fast-oxidative IIA fibers) as compared with that in the BALB/c line (38% type I fibers, 60% type IIA fibers). In contrast, these fibers had even slower oxidative phenotype than the control fibers. The fiber type composition we detected in BALB/c SOL is in agreement with the literature (Freitas et al. 2002; Luedecke et al. 2004) and represents a fiber ratio typical of a wild-type SOL, with less than 40% slow-type I fibers (Pellegrino et al. 2005; Bloemberg et al. 2012; McKeehen et al. 2013). Therefore, it is unlikely that the BALB/c mouse was not an appropriate type of control for our experiments in this regard. Based on the literature, the more than 50% slow-type I fibers in *Cmpt* animals is rather unusual for a SOL muscle in any type of mice, and is different from earlier reports on myostatin KO mice (Girgenrath et al. 2005; Gentry et al. 2011; Wang et al. 2012). This suggests that the different mechanisms of myostatin deficiency—with or without the influence of modifier genes—may induce differential and muscle-specific effects.

In summary, *Cmpt* mouse, in spite of its complex genetic background, shows similarities (at least in fast muscles) to myostatin KO mice in terms of muscle cellularity and glycolytic muscle phenotype, suggesting that the lack of myostatin is responsible for these morphological/functional changes. However, based on the more pronounced hyperplasia in *Cmpt* fast muscles as well as the different cellularity and oxidative phenotype of *Cmpt* SOL, additional studies are needed to elucidate the molecular mechanisms of myostatin inactivity and the possible role of modifier genes in *Cmpt* mice.

Acknowledgments

We thank to Makráné Felhő Zita and Balásházi Istvánné for technical assistance.

Declaration of Conflicting Interests

The author(s) declared no potential conflicts of interest with respect to the research, authorship, and/or publication of this article.

Funding

The author(s) disclosed receipt of the following financial support for the research, authorship, and/or publication of this article: This work was supported by the Hungarian National Development Agency, the European Union and co-funded by the European Social Fund [project numbers: TÁMOP 4.2.2/B-10/1-2010-0012; TÁMOP 4.2.2.A-11-1-KONV-2012-0035] and by "National Excellence Program" [TÁMOP 4.2.4.A/2-11-1-2012-0001].

References

1. Amthor H, Macharia R, Navarrete R, Schuelke M, Brown SC, Otto A, Voit T, Muntoni F, Vrbóva G, Partridge T, Zammit P, Bünger L, Patel K. 2007. Lack of myostatin results in excessive muscle growth but impaired force generation. Proc Natl Acad Sci. 104:1835–1840.
2. Amthor H, Otto A, Vulin A, Rochat A, Dumonceaux J, Garcia L, Mouisel E, Hourdé C, Macharia R, Friedrichs M, Relaix F, Zammit PS, Matsakas A, Patel K, Partridge T. 2009. Muscle hypertrophy driven by myostatin blockade does not require stem/precursor-cell activity. Proc Natl Acad Sci. 106:7479–7484.
3. Bloemberg D, Quadrilatero J. 2012. Rapid determination of myosin heavy chain expression in rat, mouse and human skeletal muscle using multicolor immunofluorescence analysis. Plos One. 7:1–11.
4. Boman IA, Klemetsdal G, Blichfeldt T, Nafstad O, Vage DI. 2009. A frameshift mutation in the coding region of the myostatin gene (MSTN) affects carcass conformation and fatness in Norwegian white sheep (Ovis aries). Anim Genetics. 40:418–422.
5. Bünger L, Laidlaw AH, Bulfield G, Eisen EJ, Medrano JF, Bradford GE, Prichner F, Renne U, Schlote W, Hill WG. 2001. Inbred lines of mice derived from long-term on growth selected lines: unique resources for mapping growth genes. Mamm Genome. 12:678–686.
6. Bünger L, Ott G, Varga L, Schlote W, Rehfeldt C, Williams JL, Hill WG. 2004. Marker assisted introgression of the Compact mutant myostatin allele: $Mstn^{Cmpt\text{-}dl1Abc}$ into a mouse line with extreme growth-effects on body composition and muscularity. Genet Res. 84:161–173.
7. Carlson CJ, Booth FW, Gordon SE. 1999. Skeletal muscle myostatin mRNA expression is fiber-type specific and increases during hindlimb unloading. Am J Physiol. 277:R601–606.
8. Clop A, Marcq F, Takeda H, Pirottin D, Tordoir X, Bibé B, Bouix J, Caiment F, Elsen JM, Eychenne F, Larzul C, Laville E, Meish F, Milenkovic D, Tobin J, Charlier C, Georges M. 2006. A mutation creating a potential illegitimate microRNA target site in the myostatin gene affects muscularity in sheep. Nat Genet. 38:813–818.
9. Freitas EM, Dal Pai Silva M, da Cruz-Höfling MA. 2002. Histochemical differences in the responses of predominantly fast-twitch glycolytic muscle and slow-twitch oxidative muscle to veratrine. Toxicon. 40:1471–1481.
10. Gentry BA, Ferreira JA, Phillips CL, Brown M. 2011. Hindlimb skeletal muscle function in myostatin-deficient mice. Muscle Nerve. 43:49–57.
11. Girgenrath S, Song K, Whittemore LA. 2005. Loss of myostatin expression alters fiber-type distribution and expression of myosin heavy chain isoforms in slow- and fast-type skeletal muscle. Muscle Nerve. 31:34–40.
12. Grobet L, Martin LJ, Poncelet D, Pirottin D, Brouwers B, Riquet J, Schoeberlein A, Dunner S, Ménissier F, Massabanda J, Fries R, Hanset R, Georges M. 1997. A deletion in the bovine myostatin gene causes the double-muscled phenotype in cattle. Nat Genet. 17:71–74.
13. Hennebry A, Berry C, Siriett V, O'Callaghan P, Chau L, Watson T, Sharma M, Kambadur R. 2009. Myostatin regulates fiber-type composition of skeletal muscle by regulating MEF2 and MyoD gene expression. Am J Physiol Cell Physiol. 296:C525–534.
14. McKeehen JN, Novotny SA, Baltgalvis KA, Call JA, Nuckley DJ, Lowe DA. Adaptation of mouse skeletal muscle to low-intensity vibration training. 2013. Med Sci Sports Exerc. 45:1051–1059.
15. McPherron AC, Lawler AM, Lee SJ. 1997. Regulation of skeletal muscle mass in mice by a new TGF-β superfamily member. Nature. 387:83–90.
16. McPherron AC, Lee SJ. 1997. Double muscling in cattle due to mutations in the myostatin gene. Proc Natl Acad Sci. 94:12457–12461.
17. Mendler L, Zádor E, Ver Heyen M, Dux L, Wuytack F. 2000. Myostatin levels in regenerating rat muscles and in myogenic cell cultures. J Muscle Res Cell Motil. 21:551–563.
18. Mosher DS, Quignon P, Bustamante CD, Sutter NB, Mellersh CS, Parker HG, Ostrander EA. 2007. A mutation in the myostatin gene increases muscle mass and enhances racing performance in heterozygote dogs. PloS Genetics. 0779–0786.
19. Pellegrino MA, Brocca L, Dioguardi FS, Bottinelli R, D'Antona G. 2005. Effects of voluntary wheel running and amino acid supplementation on skeletal muscle of mice. Eur J Appl Physiol. 93:655–664.
20. Ploquin C, Chabi B, Fouret G, Vernus B, Feillet-Coudray C, Coudray C, Bonnieu A, Ramonatxo C. 2012. Lack of myostatin alters intermyofibrillar mitochondria activity, unbalances redox status, and impairs tolerance to chronic repetitive contractions in muscle. Am J Physiol Endocrinol Metab. 302:E1000–1008.
21. Rehfeldt C, Ott G, Gerrard DE, Varga L, Schlote W, Williams JL, Renne U, Bünger L. 2005. Effects of the Compact mutant myostatin allele $Mstn^{Cmpt\text{-}dl1Abc}$ introgressed into a high growth mouse line on skeletal muscle cellularity. J Muscle Res Cell Mot. 26:103–112.
22. Savage KJ, McPherron AC. 2010. Endurance exercise training in myostatin null mice. Muscle Nerve. 42:355–362.
23. Schuelke M, Wagner KR, Stolz LE, Hübner C, Riebel T, Komen W, Braun T, Tobin JF, Lee SJ. 2004. Myostatin mutation associated with gross muscle hypertrophy in a child. New Engl J Med. 350:2682–2688.
24. Stinckens A, Luyten T, Bijttebier J, Van den Maagdenberg K, Dieltiens D, Janssens S, De Smet S, Georges M, Buys N. 2008. Characterization of the complete porcine MSTN gene and expression levels in pig breeds differing in muscularity. Anim Genet. 39:586–596.
25. Szabó G, Dallmann G, Müller G, Patthy L, Soller M, Varga L. 1998. A deletion in the myostatin gene causes the compact

(Cmpt) hypermuscular mutation in mice. Mamm Genome. 9:671–672.
26. Valle Zarate A, Horst P, Weniger JH. 1994. Antagonism Between Growth and Productive Adaptability in Mice. Archiv für Tierzucht-Archives of Animal Breeding. 37:185–198.
27. Varga L, Szabó G, Darvasi A, Müller G, Sass M, Soller M. 1997. Inheritance and mapping of Compact (Cmpt), a new mutation causing hypermuscularity in mice. Genetics. 147:755–764.
28. Varga L, Müller G, Szabó G, Pinke O, Korom E, Kovács B, Patthy L Soller M. 2003. Mapping modifers affecting muscularity of the myostatin mutant ($Mstn^{Cmpt\text{-}dl1Abc}$) Compact mouse. Genetics. 165:257–267.
29. Varga L, Pinke O, Müller G, Kovács B, Korom E, Szabó G, Soller M. 2005. Mapping a syntenic modifier on mouse chromosome 1 influencing the expressivity of the Compact phenotype in the myostatin mutant ($Mstn^{Cmpt\text{-}dl1Abc}$) Compact mouse. Genetics. 169:489–493.
30. Wang M, Yu H, Kim YS, Bidwell CA, Kuang S. 2012. Myostatin facilitates slow and inhibits fast myosin heavy chain expression during myogenic differentiation. Biochem Biophys Res Commun. 426:83–88.
31. Wegner J, Albrecht E, Fiedler I, Teuscher F, Papstein HJ, Ender K. 2000. Growth and breed-related changes of muscle fiber characteristics in cattle. J Anim Sci. 78:1485–1496.
32. Weniger JH, Horst P, Steinhauf D, Major F, Wolf M, Tawfik ES. 1974. Model experiments on selection for endurance and its relation to growth. Part I. Introduction, methods and preliminary investigations on the basic population. Journal of Animal Breeding and Genetics-Zeitschrift für Tierzüchtung und Züchtungsbiologie. 91:265–270.